Faculty of Design, Industrial Design, Inclusive Design, Perceptual Artifacts Lab (PAL)

2021

Spectral landscapes of flow instabilities in brain aneurysms

Natarajan, Thangam, MacDonald, Daniel E., Temor, Lucas, Coppin, Peter W. and Steinman, David A.

Gallery of Fluid Motion

Spectral landscapes of flow instabilities in brain aneurysms

Thangam Natarajan,[1] Daniel E. MacDonald,[1] Lucas Temor,[1]
Peter W. Coppin,[2] and David A. Steinman[1,*]
[1]*Department of Mechanical and Industrial Engineering, Biomedical Simulation Laboratory, University of Toronto, Toronto, Ontario, Canada*
[2]*Perceptual Artifacts Laboratory, OCAD University, Toronto, Ontario, Canada*

(Received 6 August 2021; published 15 November 2021)

This paper is associated with a poster winner of a 2020 American Physical Society's Division of Fluid Dynamics (DFD) Milton van Dyke Award for work presented at the DFD Gallery of Fluid Motion. The original poster is available online at the Gallery of Fluid Motion, https://doi.org/10.1103/APS.DFD.2020.GFM.P0004.

DOI: 10.1103/PhysRevFluids.6.110505

Rupture of a brain aneurysm (local bulging of arteries in the brain) is a devastating event, leading to death or permanent disability in the majority of cases. Roughly 1 in 30 adults harbor a brain aneurysm and unruptured aneurysms are being detected more frequently due to the growing use of three-dimensional (3D) medical imaging. Our research focuses on the use of "patient-specific" computational fluid dynamics (CFD) to help doctors decide whether and how to treat an unruptured aneurysm since the risk of treating can often outweigh the risk of rupture. This poster describes how our team of engineers and designers are using machine learning and perceptual-cognitive principles to make sense of the large amounts of clinical CFD data we generate, in order to identify which kinds of fluid dynamic features within the aneurysm sac may make it prone to rupture.

"Turbulent-like" blood flow is thought to be an important factor in the risk assessment and treatment planning of patients with brain aneurysms [1]. Towards making sense of large patient-derived CFD datasets, we present an illustration-inspired visualization of these hemodynamics and their spectral characteristics sorted by a neural network.

Figure 1(a) shows one potential location of a brain aneurysm within the cerebral vasculature. As a part of the diagnosis, medical imaging of the vasculature is carried out through 3D angiography. The aneurysm and proximal segments of vasculature are then carefully segmented to obtain 3D surface models. In the current paper, we used 50 such patient-specific models from the open-source Aneurisk data repository [2].

High-fidelity CFD was performed for each of these models using meshes that consisted of 3×10^6 quadratic elements on average for 20 000 time steps per cardiac cycle (0.951 s). Fully developed physiologically accurate velocity was imposed at the inlet, and physiological flow splits were applied at the outlets. Simulations were performed with a well-validated minimally dissipative finite-element solver. For more detailed simulation parameters and meshing details, see Khan *et al.* [3]. The impact of various parameters and the uncertainties associated at every stage and their impact on the pulsatile hemodynamics are discussed in Steinman and Periera [4].

*Corresponding author: steinman@mie.utoronto.ca

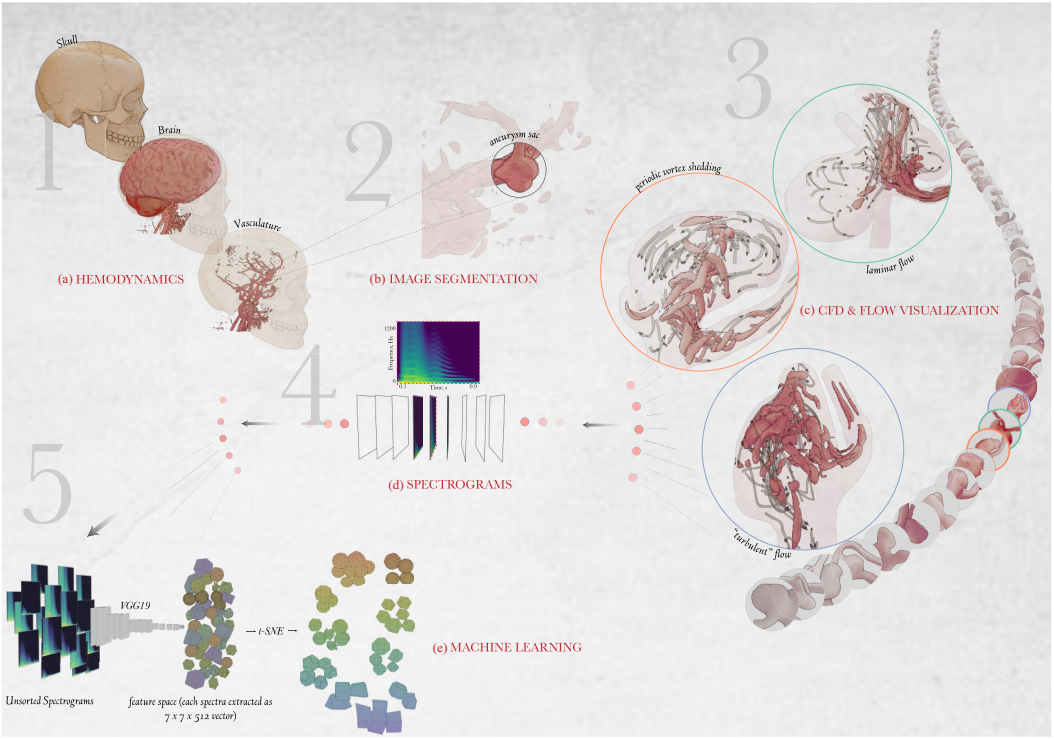

FIG. 1. Snapshot of pre- and post-processing of aneurysm models and their CFD data.

With recent reports uncovering the presence of high frequency (on the order of 100 s of hertz) flow instabilities in the aneurysms—which previously were modeled as laminar—we are interested in characterizing the nature of these flows both qualitatively and quantitatively. In Fig. 1(c), all 50 aneurysm models are shown as a "swoosh" and isosurfaces of a Q criterion for three representative cases are shown for flow phenotypes ranging from smooth laminar flow to vortex shedding to turbulentlike flows [5]. The path lines embedded within the Q criterion provide a context of the complexity of the flow within the sac of the aneurysm. The Q criterion and path lines were computed with the open-source software PARAVIEW [6] and were rendered in BLENDER [7].

To understand the harmonic complexity in these flows, we chose spectrograms since they provide a comprehensive yet short-hand representation of the overall spectral content in the CFD model. Spectrograms [Fig. 1(d)] were generated via short-time Fourier transforms of the velocity-time data within the aneurysm sac region of each simulation [8]. In the broadest sense, the spectrogram is a visual representation of the evolution of spectral content of time-series data, essentially mapping the power of the signal to color and/or intensity in a time-frequency plane. All the cases simulated with 20 000 saved time steps per cardiac cycle would, in principle, allow us to analyze frequencies up to 10.5 kHz, and the sampling rate would be 21 kHz. In practice, however, snapshots are typically saved for only a subset of (typically equal-spaced) time steps to minimize storage and reduce I/O bottlenecks. In our case we typically write only 1250–2500 snapshots/cycle, i.e., allowing us to resolve frequencies up to 0.6–1.3 kHz. Together with the Q criterion, these provide a rich representation of the frequencies and duration of flow disturbances in the patient cohort, but as a group they are visually dense and difficult to classify manually.

Once the spectrograms are obtained, it is of course possible to go through each of these 50 cases and comprehend the nature of these flows. However, this is time consuming and certainly an information overload for the viewer to account for all the cases and see their inter- and

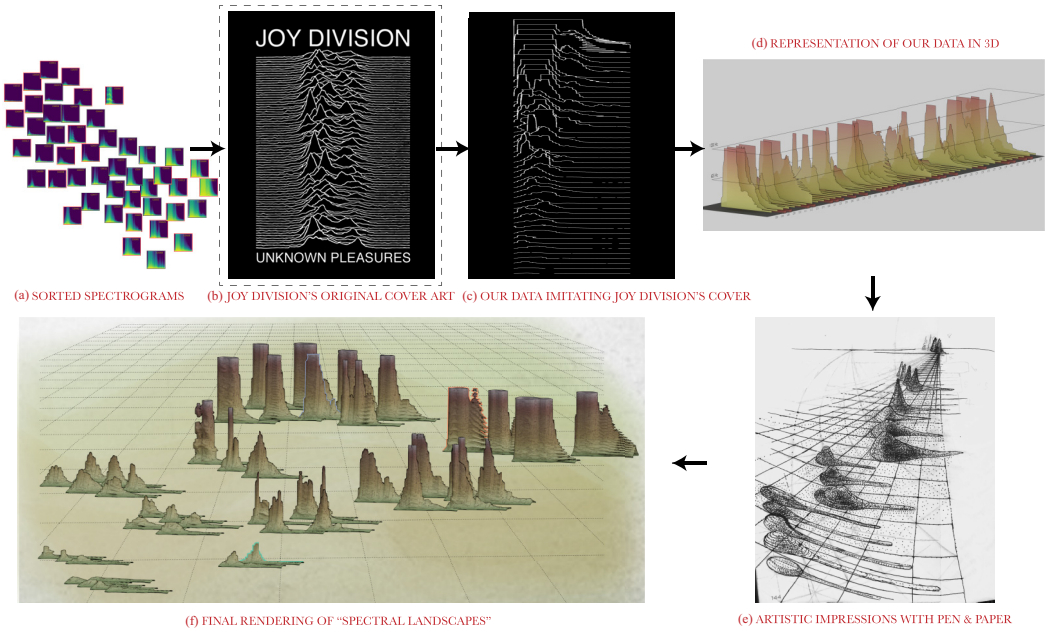

FIG. 2. A snapshot of the creative process in arriving at the final representation.

intra-relationships. To overcome this arduous manual labor, we addressed the issue in two stages. First, it would be intuitive to group these large datasets based on a representative proxy for the four-dimensional flow field. Second, once they are grouped, there still is a need to present these 50 spectrograms in a digestible format or a representation such that the user can focus on all the cases simultaneously and still consume the information these spectrograms have to offer. To address the first issue, we adapted machine learning algorithms to sort and cluster the spectrograms from all the cases investigated. To address the second issue of representing all the cases, we used illustration-inspired and perceptual-cognitive principles as discussed later.

The process of sorting the spectrograms using deep convolutional neural networks (CNNs) is shown in Fig. 1(e). To sort spectrograms by similarity, we took a two-step approach similar to Karpathy [9]: (i) CNN to extract high-dimensional abstract features from each spectrogram; (ii) passing these feature representations to a dimensionality reduction algorithm t-distributed stochastic neighbor embedding (t-SNE).

The chosen CNN is a pretrained VGG19 network obtained from PyTorch Hub and can be readily downloaded from an online portal [10]. The network was trained to classify images using the IMAGENET database of over 14×10^6 natural images. Such pretrained networks are commonly used for benchmarking learning tasks or for transfer learning by retraining only select network layers, thereby leveraging the considerable training time already imparted to the network. Since we are interested only in the feature-extraction capability of the network (and not the final classification or class-specific features) we pass each spectrogram through only the first 15 layers of VGG19 at which point a high-dimensional feature-space object (tensor) is extracted. Input images with similar visual features will have similar feature-space representations.

These high-dimensional feature-space objects are not human interpretable; to visualize the similarity between images, we use t-SNE to construct a two-dimensional (2D) embedding that respects the high-dimensional distances between the feature-space objects. Visualizing the plane of this embedding [Fig. 2(a)], spectrograms that appear near to each other are also nearby in the high-dimensional feature space representation. The t-SNE algorithm is not deterministic, so

embeddings may be different depending on input data and algorithm hyperparameters and may not be appropriate for downstream classification tasks; Fig. 2(a) shows one representative example of a 2D embedding of the 50 spectrograms as generated using t-SNE. This method gives visually pleasing results, separating spectra distinctly by spectral envelope with some consideration for harmonic bandedness, the latter suggesting the presence of laminar vortex shedding phenomena vs turbulence.

The t-SNE-sorted spectrograms provide a broad categorization of the models based on the features extracted from the spectrogram. Figure 2 shows the creative process we underwent to arrive at the final representation of all the cases. In Fig. 2(a) we have all the spectrograms grouped based on the features. To represent all the spectra, we initially tried to represent them as 2D "joy division plots" as shown in Figs. 2(b) and 2(c). Although we could fairly represent all the cases, conveying the classification of these spectrograms was still a challenge. We moved to 3D representations [Fig. 2(d)] of these spectrograms to add more depth cues within these spectrograms. However, occlusion was apparent and we needed a perceptually optimized view to represent the spectra. Artistic impressions [Fig. 2(e)] suggested that with a suitable projection of the view, the desired representation could be achieved. Inspired by mountainous landscapes, Fig. 2(f) shows the final version of "spectral landscape" used in the poster.

To amplify their appearance, spectrograms were extruded in 3D and shown in perceptually optimized [11] landscape to visualize all 50 cases simultaneously, whereas also being able to discern the presence and nature of the (time-varying) flow instabilities. Spectral "lowlands" correspond to cases with low-frequency (laminar) flows. Progressively higher "mountain ranges" represent clusters of cases having similar intensity and harmonic content of flow instabilities: terraces indicate the presence and nature of narrow-band (vortex-shedding) phenomena, whereas weathering indicates broadband (more turbulentlike) flows. The persistence of flow disturbances into the cardiac cycle is indicated by the horizontal extent of the peaks, whereas plateaus reflect the unavoidable clipping of our dense CFD data files at a ($\sim$1.3-kHz) Nyquist limit. Note the three highlighted cases, corresponding to the laminar, vortex-shedding and turbulent flow cases highlighted above.

To summarize, towards making sense of large patient-derived CFD datasets, we present an illustration-inspired visualization of these hemodynamics and their spectral characteristics sorted by a neural network. Together these techniques enabled the visualization of 50 cases and the broad nature of their flow characteristics in a perceptually optimized and intuitive manner.

We acknowledge the funding from the Natural Sciences and Engineering Research Council of Canada and the Research Council of Norway and support of Dr. K. Valen-Sendstad from Simula Research Laboratory.

[1] K. Valen-Sendstad and D. A. Steinman, Mind the gap: impact of computational fluid dynamics solution strategy on prediction of intracranial aneurysm hemodynamics and rupture status indicators, Am. J. Neuroradiology **35**, 536 (2014).

[2] Aneuriskweb, the aneurisk dataset repository, http://ecm2.mathcs.emory.edu/aneuriskweb/index. Accessed: 2021-08-03.

[3] M. O. Khan, V. T. Arana, M. Najafi, D. E. MacDonald, T. Natarajan, K. Valen-Sendstad, and D. A. Steinman, On the prevalence of flow instabilities from high-fidelity computational fluid dynamics of intracranial bifurcation aneurysms, J. Biomech. **127**, 110683 (2021).

[4] D. A. Steinman and V. M. Pereira, How patient specific are patient-specific computational models of cerebral aneurysms? An overview of sources of error and variability, Neurosurgical Focus **47**, E14 (2019).

[5] T. Natarajan, D. E. MacDonald, M. Najafi, P. W. Coppin, and D. A. Steinman, Spectral decomposition and illustration-inspired visualisation of highly disturbed cerebrovascular blood flow dynamics, Comput. Methods Biomech. Biomed. Eng.: Imaging Vis. **8**, 182 (2020).
[6] U. Ayachit, *The ParaView Guide: A Parallel Visualization Application* (Kitware, Inc., New York, 2015).
[7] Blender Online Community, *Blender-A 3D Modelling and Rendering Package* (Blender Foundation, Blender Institute, Amsterdam, 2017).
[8] T. Natarajan, D. E. MacDonald, M. Najafi, M. O. Khan, and D. A. Steinman, On the spectrographic representation of cardiovascular flow instabilities, J. Biomech. **110**, 109977 (2020).
[9] t-SNE visualization of CNN codes, https://cs.stanford.edu/people/karpathy/cnnembed/. Accessed: 2021-08-03.
[10] PyTorch VGG-NETS, https://pytorch.org/hub/pytorch_vision_vgg/. Accessed: 2021-08-03.
[11] D. A. Steinman, P. W. Coppin, and D. A. Steinman, Narcissus and echo: Reflections on an art-science collaboration, Leonardo **54**, 552 (2021).